Zoosyst. Evol. 100 (1) 2024, 69–85 | DOI 10.3897/zse.100.112778

PENSOFT

MUSEUM FÜR NATURKUNDE BERLIN

Population variation of *Diapoma pampeana* (Characiformes, Characidae, Stevardiinae) from an isolated coastal drainage in Uruguay, with new records: comparing morphological and molecular data

James Anyelo Vanegas-Ríos[1], Wilson Sebastián Serra Alanís[2,3], María de las Mercedes Azpelicueta[1], Thomas Litz[4], Luiz Roberto Malabarba[5]

1 *División Zoología Vertebrados, Facultad de Ciencias Naturales y Museo, Unidades de Investigación Anexo Museo, Gabinete 104, CONICET, UNLP, La Plata, Buenos Aires, Argentina*

2 *Sección Ictiología, Departamento de Zoología, Museo Nacional de Historia Natural, Montevideo, Uruguay*

3 *Centro Universitario Regional del Este (CURE) Sede Rocha, Rocha, Uruguay*

4 *Friedhofstr. 8, 88448 Attenweiler, Germany*

5 *Laboratório de Ictiologia, Departamento de Zoologia, Universidade Federal do Rio Grande do Sul (UFRGS), Av. Bento Gonçalves, 9500, 91501-970 Porto Alegre, RS, Brazil*

https://zoobank.org/BAC6CFC9-E0EC-459A-9A7B-18F0A5F71D68

Corresponding author: James Anyelo Vanegas-Ríos (anyelovr@fcnym.unlp.edu.ar)

Academic editor: Nicolas Hubert ♦ **Received** 20 September 2023 ♦ **Accepted** 8 December 2023 ♦ **Published** 26 January 2024

Abstract

Diapoma pampeana was recently described to occur in the upper Negro basin in Uruguay and Brazil. An isolated population tentatively identified as *D. pampeana* from the Pando stream, a perturbed coastal drainage in Uruguay, is studied and compared under the light of morphological and molecular data to test if there is evidence to consider it as a separate species. New geographical records for the species are presented and included in the comparisons. The specimens analyzed were pooled into four groups: Pando, Santa Lucía, Middle Negro and Upper Negro. We analyzed 32 morphological characters using statistical procedures and recovered a COI-based phylogeny of different populations of *D. pampeana* to test if they may represent different species. Size-corrected PCA revealed that the Pando and Upper Negro groups are greatly diverging in both morphometric and meristic data along PC1 (mainly by the snout to dorsal-fin origin, dorsal to adipose-fin origins, number of longitudinal scales and predorsal scales). This deviating pattern was also obtained in a cluster analysis. The Santa Lucía and Middle Negro groups were found to be intermediate morphotypes. In contrast, molecular analyses revealed that the Pando and Upper Negro specimens resemble genetically and, thus, are placed together in the Neighbor-joining and Bayesian topologies, as part of a monophyletic *Diapoma*. We proposed that the Pando population, despite its deviating morphology observed, can be classified as *D. pampeana*. Therefore, this population constitutes a remarkable example of an isolated population that is morphologically divergent but genetically similar to the geographically most distant conspecific population.

Key Words

Body shape variation, integrative taxonomy, Neotropical fish, phylogeny, size-corrected PCA

Introduction

The Neotropical fish genus *Diapoma* Cope, 1894 is a member of the tribe Diapomini, which is one of the largest monophyletic groups within the Stevardiinae with ~ 135 relatively small-sized species (no more than 100 mm SL) (Thomaz et al. 2015; Mirande 2019; Ferreira et al. 2021; Ito et al. 2022; Fricke et al. 2023). *Diapoma* is recognized as a monophyletic group based on molecular data and combined evidence (Thomaz et al. 2015; Mirande 2019; Ito et al. 2022).

To date, this genus includes sixteen valid species that are distributed along different river drainages in Argentina, Brazil, Paraguay and Uruguay, mainly within the Rio de la Plata basin. Five species are known from the Paraná-Paraguay system, *D. guarani* (Mahnert & Géry, 1987) (several streams flowing into the Paraná basin in the border region between Alto Paraná, Paraguay and Misiones, Argentina), *D. obi* (Casciotta, Almirón, Piálek & Rícan, 2012) (some tributaries from the Paranay-Guazú drainage and the Moreno stream in Misiones, Argentina), *D. nandi* Vanegas-Ríos, Azpelicueta & Malabarba, 2018 (the Piray-Miní stream in Misiones, Argentina), the recently described *D. potamohadros* Ito, Carvalho, Pavanelli, Vanegas-Ríos & Malabarba, 2022 (endemic from the Rio Iguazú basin in Argentina and Brazil) and *D. terofali* (Géry, 1964) (the Rio Luján and other streams flowing into the Rio de la Plata basin in Buenos Aires, Argentina) (Mahnert and Géry 1987; Menezes and Weitzman 2011; Casciotta et al. 2012; Vanegas-Ríos et al. 2018; Ito et al. 2022). The Rio Uruguay basin is the water body that possesses the greater number of *Diapoma* species registered so far (seven spp.), *D. alegretense* (Malabarba & Weitzman, 2003) (the Rio Ibicuí system in Rio Grande do Sul, Brazil, and Laguna Redonda in Artigas, Uruguay), *D. guarani* (Barragem Sanchuri in Rio Grande do Sul, Brazil), *D. lepiclastum* (Malabarba, Weitzman & Casciotta, 2003) (from the Rio Pelotas and Rio Canoas to the Lageado União stream in Brazil, and in the eastern region of Misiones, Argentina), *D. pampeana* Ito, Carvalho, Pavanelli, Vanegas-Ríos & Malabarba, 2022 (the upper Rio Negro basin in Brazil and Uruguay), *D. pyrrhopteryx* Menezes & Weitzman, 2011 (the Rio Pelotas basin in Rio Grande do Sul, Brazil, and the Pepirí Iguazú basin in Misiones, Argentina), *D. terofali* (streams flowing into the Rio Uruguay system in Río Grande do Sul, Brazil, and in Artigas and Cerro Largo, Uruguay), and *D. uruguayense* (Messner, 1962) (tributaries of the Rio Uruguay in the border region between Argentina, Uruguay, and Brazil, and from the headwaters of the Rio Negro) (Malabarba and Weitzman 2003; Zarucki et al. 2010; Menezes and Weitzman 2011; Thomaz et al. 2015; Almirón et al. 2016). Four species have been recorded for the Laguna dos Patos basin and the coastal drainages of south Brazil, *D. dicropotamicum* (Malabarba & Weitzman, 2003) (northern tributaries of the Rio Jacuí from the Serra Geral formation), *D. itaimbe* (Malabarba & Weitzman, 2003) (Tramandaí, Mampituba, Araranguá river basins, southern coast of Brazil), *D. speculiferum* Cope, 1894, *D. thauma* Menezes & Weitzman, 2011 (tributaries of the Rio Jacuí basin, Rio Grande do Sul, Brazil) and *D. tipiaia* (Malabarba & Weitzman, 2003). Finally, *D. alburnum* (Hensel, 1870) is the most widely distributed species occurring in the Uruguay (e.g. the Rio Queguay basin), Paraná (the Río Gualeguay basin), Laguna dos Patos (e.g. the Rio Jacuí system) basins and coastal drainages of southern Brazil (Malabarba 1983; Malabarba and Weitzman 2003; Protogino and Miquelarena 2012; Paullier et al. 2019).

Diapoma pampeana, recently described from the upper Rio Negro basin, reaches 35 mm SL and can be differentiated from all its congeners by a combination of characters, mainly from body pigmentation (Ito et al. 2022), including the presence of: a narrow and conspicuous black line along the horizontal septum, never forming a wide lateral stripe; a longitudinal black stripe extending posteriorly on the middle caudal-fin rays; and a small black blotch, restricted to the base of the middle caudal-fin rays.

We found specimens that potentially could be identified as *D. pampeana* from the Pando stream, a coastal drainage flowing into the Rio de la Plata estuary in Uruguay, based on the resemblance of the humeral mark, midlateral stripe, and caudal-fin pigmentation. The possible presence of this species in the Pando stream caught our attention because the preliminary morphometric data obtained were somewhat incongruent with the data reported in the description by Ito et al. (2022), and because no congener has been recorded in this area so far (Malabarba and Weitzman 2003; Menezes and Weitzman 2011; Gurdek and Acuña-Plavan 2017). This small drainage, which is located in the middle of urban and agricultural areas, has been greatly modified and affected by anthropogenic factors such as pollution, industrial activities, and urban waste originated from anthropogenic actions (Echevarría et al. 2011; Achkar et al. 2012; Gutiérrez et al. 2015; Muniz et al. 2019) and is considered of great importance, among other reasons, because its sub-estuarine mouth plays a role in the breeding and nursery for grounds of fish (Defeo et al. 2009; Acuña et al. 2017; Muniz et al. 2019).

There are several studied cases in which species previously considered as distributed in the Rio Uruguay drainage and Atlantic river coastal drainages have been separated in two different species [e.g. *Parapimelodus nigribarbis* (Boulenger, 1889) vs. *P. valenciennis* (Lütken, 1874), see Lucena et al. (1992); *Pimelodus pintado* Azpelicueta, Lundberg & Loureiro, 2008 vs. *P. maculatus* Lacepède, 1803, see Azpelicueta et al. (2008); *Bunocephalus erondinae* Cardoso, 2010 vs. *B. doriae* Boulenger, 1902, see Cardoso (2010); *Pseudocorynopoma stanleyi* Malabarba, Chuctaya, Hirschmann, Oliveira & Thomaz, 2020 vs. *P. doriae* Perugia, 1891, see Malabarba et al. (2021)]. So, the present study aims to carry out a morphological (mainly morphometric and meristic data) and COI-based comparison between the population of *D. pampeana* from the Rio Negro basin, a tributary of the lower Rio Uruguay, and the population tentatively identified as *D. pampeana* from the Pando stream, that empties directly in the Atlantic Ocean. We expect to test if there is evidence to consider these isolated populations as separate species or to treat them as a single species, describing any intraspecific variation between them. Additionally, a recent examination of specimens of *Diapoma* at Museo Nacional de Historia Natural, Montevideo (MHNM), revealed two lots of individuals similar to *D. pampeana* in the body shape and meristic data from the Yi and Santa Lucía river basins (as fixed in 10% formalin, DNA extraction was unavailable). Consequently, they were included in the morphological analyses to enhance the comparisons and are also presented as new records.

Materials and methods

Specimens were collected in the Pando stream (permission No. 202/717/04, DINARA, Uruguay) between 2003 and 2004. They were fixed in formalin 10% and preserved in alcohol 70%. Some of them, which were preserved originally in ethanol 96%, were rehydrated before being preserved and catalogued as the others. Additional studied specimens of *D. pampeana* and comparative species are deposited in the following institutions: MACN-ict, MLP, MHNG, MHNM, UFRGS, and UNMDP (abbreviations according to Sabaj 2020).

Morphological analysis

Measurements and other counts were taken following Fink and Weitzman (1974), with the modifications presented by Ito et al. (2022). Twenty-two measurements were taken point to point with a digital caliper under a stereomicroscope and are expressed as percentages of standard length (SL) or head length (HL) for units of the head. Specimens were cleared and stained (c&s) following Taylor and Dyke (1985). The total number of vertebrae was counted in c&s specimens. Those counts included the first preural centrum plus the first ural centrum (PU1 + U1) counted as one element and all four vertebrae of the Weberian apparatus.

The specimens from the Pando stream were compared with type specimens of *D. pampeana* from the Rio Negro basin under different statistical procedures. Additionally, the specimens presumably belonging to *D. pampeana* from the Yi and Santa Lucía river basins in Uruguay were only processed in the morphological analyses because they were not suitable for DNA extraction. To facilitate comparisons, a morphometric data matrix that included all of these specimens was pooled into groups (based on geographic drainages) as follows: Pando (n = 17), Santa Lucía (Canelón Grande, n = 2), Middle Negro (Yi, n = 15), and Upper Negro (several localities, n = 35). Nearly all the specimens analyzed in all groups were adults, except for a few immature specimens that were also added in the comparisons (excluding the bone hooks, no morphometric or meristic differences were observed between them and the respective adults). This dataset was analyzed using the "allometric vs. standard" procedure (Elliott et al. 1995), under which the allometric coefficients are calculated concerning a standard (reference, such as overall length) measurement (each variable is regressed onto this after log-transformation). The size-corrected morphometric dataset was analyzed using a principal component analysis (PCA), based on the covariance matrix. For the PCA, the number of significant principal components (PCs) was decided by two criteria: the broken-stick model (Frontier 1976) and the scree plot method (Cattel 1966). To compare the dissimilarity between the groups associated with the size-corrected morphometric data, a hierarchical cluster analysis was performed using Ward's method (Ward 1963) and Euclidean distances, under 1000 bootstrap replicates. Missing values in measurements (e.g. some fin rays were broken in a few individuals) were imputed from predictor values obtained under maximum likelihood from the EM algorithm (Dempster et al. 1977; Pigott 2001) using 500 iterations. For the morphometric data, confidence intervals of 95% were calculated using 9000 bootstraps.

Meristic data showing slightly different patterns between the Pando group and the other groups were analyzed using a PCA on the root-squared transformed values and the correlation matrix (Quinn and Keough 2002) (outliers that could not be reexamined in the specimens were omitted and the mean was imputed for missing data). To illustrate the distinctive patterns within the Pando group, we used Tukey box plots for the variables, which provide a clearer representation of the observed variability. When it comes to counts, both mean and mode values are reported, and they are separated by a slash.

For those analyses, normality was tested using a Shapiro–Wilk statistic (W) in each case ($\alpha < 0.05$) and data were log-transformed when needed to better approximate to a multivariate normality. Statistical procedures were carried out in PAST 4.12 (Hammer et al. 2001), IBM SPSS Statistics 26.0 (IBM 2019), and GraphPad Prism 9.4.1 (GraphPad Software, San Diego, CA, USA).

Molecular analysis

The mitochondrial cytochrome c oxidase subunit I gene (COI) was obtained from two specimens from the Pando stream. DNA extraction and polymerase chain reaction (PCR) were carried out following the standard COI protocols (Ivanova et al. 2006; Rosso et al. 2012), under different sets of primer cocktails for fishes (Ivanova et al. 2007).

In total each amplification reaction produced a volume of 12.375 µL from 2 µL of DNA template, 6.25 µL of 10% trehalose, 2 µL of molecular biology grade water, 1.25 µL of 10× reaction buffer, 0.625 µL of MgCl2 (50 µM), 0.0625 µL of dNTP (10 mM), 0.0625 µL of each primer (10 µM) and 0.0625 µL of Invitrogen's Platinum Taq. polymerase (5 U µL−1). The amplification conditions consisted of 2 min at 95 °C, followed by 35 cycles at 94 °C for 30 s, at 52 °C for 40 s and at 72 °C for 1 min, and ended at 72 °C for 10 min. E-Gels (Invitrogen) were used to check the amplification success. The COI gene was sequenced in Macrogen (Korea) and IGEVET-UNLP (Argentina). Sequence chromatograms were edited using BioEdit 7.2.5 (Hall 1999).

For comparative purposes, in addition to the newly generated sequences, 72 COI sequences were selected from representative specimens of the valid species of *Diapoma* (except *D. nandi*) (Ito et al. 2022) and genera closely related to it (detailed later herein) that are available in GenBank and Barcode of Life database (BOLD, available at http://www.boldsystems.org) (accession numbers for all sequences analyzed are provided in Suppl. material 1). The COI sequences were aligned with MUSCLE (1000 iterations) (Edgar 2004) and generated as a data matrix

partitioned by the first three codon positions in MEGA 11.0.13 (Tamura et al. 2021). The COI dataset was uploaded to Zenodo (https://doi.org/10.5281/zenodo.8361520).

To analyze the phylogenetic placement of the specimens from the Pando stream through different methods, the COI data matrix was analyzed by the phylogenetic procedures and conditions described hereafter. Modeltest-NG (Darriba et al. 2019) was used for selecting the best-fit nucleotide substitution model available for each procedure (and computational package) based on the partitioned alignment when necessary. The AIC and BIC statistical criteria were explored, but the latter was used to choose the best model among the candidate models. The neighbor-joining (NJ) tree (10000 bootstrap) was constructed based on the Tajima+Nei model with rates gamma-distributed as implemented in Mega. Bayesian analyses were conducted in MRBAYES 3.2.2 (Ronquist et al. 2012) using two runs, each with four Markov chains, which ran for 60 million generations (25% discarded as burn-in, sampling a tree every 3000 generations) under the models SYM+I (position 1), F81 (position 2) and HKY+G (position 3). Tracer 1.7.2 (Rambaut et al. 2018) was used to evaluate the results of the MRBAYES analyses from each run (ESS values and lnL plots). The trees were visualized and prepared with FIGTREE 1.4.4 (Rambaut 2018). The CIPRES portal (Miller et al. 2010) was used to run the following computational programs: MODELTEST-NG and MRBAYES 3.2.2. The outgroup was composed of species from *Bryconamericus* Eigenmann, 1907, *Hypobrycon* Malabarba & Malabarba, 1994, *Nantis* Mirande, Aguilera & Azpelicueta, 2006, *Odontostoechus* Gomes, 1947, *Piabarchus* Myers, 1928, and *Piabina* Reinhardt, 1867, genera that have been considered in preceding studies (Ferreira et al. 2011; Mirande 2019; Ito et al. 2022) to be closely related to *Diapoma* (trees were rooted in *Piabina* species when required). Additionally, to compare the interspecific and within-species variability, the uncorrected pairwise genetic distances (gamma distributed and pairwise deletion) were calculated in MEGA 11.0.13 (Tamura et al. 2021).

To examine the potential variability associated with polymorphism between the Pando and Upper Negro specimens, despite the limited number of samples available, the specimens of *D. pampeana* in the COI data matrix were pooled into the two respective groups using DNASP 6.12.03 software (Rozas et al. 2017) to calculate the polymorphism sites, nucleotide diversity (π) (Nei and Li 1979), net (Da) and absolute (Dxy) divergences (Nei 1987), and to generate the haplotypes set including invariant sites and gaps. POPART (Leigh and Bryant 2015) was used to construct a haplotype network using a median-joining algorithm and default settings.

Results

Based on the comparisons carried out (detailed below), we confirmed that the examined specimens from the Pando stream (Figs 1, 2A, B), Santa Lucía system (Fig. 2C), and middle Rio Negro basin (Fig. 2E) correspond to new records of *D. pampeana*, which extend its distribution to the southwest from the upper Negro basin (in straight-line distances: ~ 200 km to Middle Negro, ~ 280 km to Santa Lucía, and ~ 290 km to Pando) (Fig. 3). The list of examined specimens of *D. pampeana* is presented in Table 1.

Morphological comparisons

The measurements of the examined specimens are summarized in Table 2. Comparing the morphometric data between the Pando group and the other groups, discrete differences between the ranges obtained were not detected. Some tendencies based on the mean in some measurements, with partially overlapping ranges, were observed. The distance between the snout and dorsal-fin origin tended to be slightly longer in the Pando, Santa Lucía and Middle Negro groups than in the Upper Negro group (53.5–58.2% SL, mean = 55.7%±1.4 in Pando; 54.2–55.7% SL, mean 54.9%±1.1 in Santa Lucía; 54.2–57.6% SL, mean = 55.8%±1.0 in Middle Negro vs. 49.0–56.2% SL, mean = 52.7%±1.7 in Upper Negro). The Pando group presented a slightly smaller distance between the dorsal- and adipose-fin origins compared to the Upper Negro group (30.4–34.8% SL, mean = 33.0%±1.1 vs. 33.0–39.9% SL, mean = 37.1%±1.4), but almost similar to the other groups (33.6–34.4 & SL, mean = 34.0±0.6 in Santa Lucía; 32.0–36.1% SL, mean = 33.9%±1.0 in Middle Negro, respectively). In other measurements, as the caudal peduncle length and snout length, the Pando group tended to show greater mean values as follow (Pando, Santa Lucía, Middle Negro and Upper Negro, respectively): for caudal peduncle length 12.1–14.6% SL, mean = 13.6%±0.7; 12.1–13.4% SL, mean = 12.8±0.9; 12.5–15.0% SL, mean = 13.4%±0.6; 8.9–13.4% SL, mean = 11.3%±1.0; and for snout length 19.3–22.3% HL, mean = 21.0%±0.8; 21.5–21.6% HL, mean = 21.5%±0.1; 20.1–22.1% HL, mean = 20.8%±0.6; 16.3–22.1% HL, mean = 19.1%±1.6.

Based on the consensus between the scree plot method and broken-stick model (Suppl. material 2), to ensure that did not discard biologically pertinent data, four eigenvector elements were selected in the PCA on the size-corrected data, which accounted for 70.7% of the total variance (Suppl. material 3; Fig. 4A, B). Along the first axis in the PC1 vs. PC2 plot (Fig. 4A: explained 53.2% of the total variance), the Pando group was almost fully differentiated from the Upper Negro group, but overlapped with the majority of the specimens of the Santa Lucía and Middle Negro groups. In the PC3 vs. PC4 plot (Fig. 4B explained 17.6% of total variance), the groups appeared to overlap, and there was no clear distinction between them. PC1 was most heavily loaded by the following measurements (Fig. 4A, Table 3): negatively by the snout to dorsal-fin origin (-0.5), snout to anal-fin origin (-0.3), caudal peduncle length (-0.3), snout to pelvic-fin origin (-0.2), and caudal peduncle depth (-0.2); and positively by the dorsal- to adipose-fin origins (0.5) dorsal fin to caudal-fin base (0.2), dorsal-fin length (0.2), and anal-fin base length (0.2). PC2 was most influenced by positive variables such

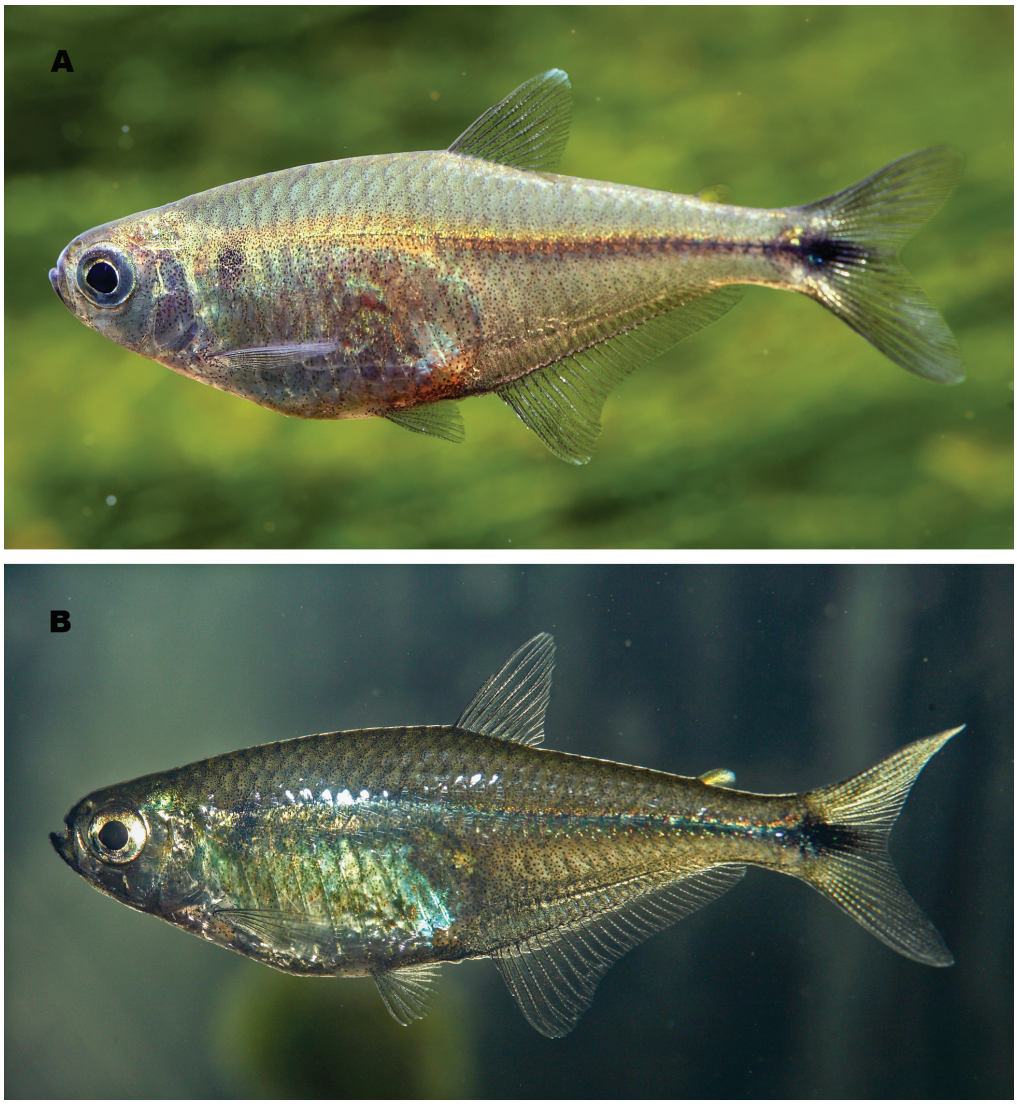

Figure 1. Coloration in life of *D. pampeana* (**A, B**) from the Pando stream, Canelones Uruguay. Photo by J. Pfleiderer.

Table 1. New records and material examined of *D. pampeana*. n = number of examined specimens. Group names corresponds with those described in the text. Accession numbers: OR533516* and OR533515**.

Group	n	SL (mm)	Catalog number	Country	Locality	Latitude/Longitude	Remarks
Santa Lucía	1	31.3	MHNM 1125	Uruguay	Canelones, Rio Santa Lucía basin, Canelón Grande stream	34°29'14.00"S, 56°20'33.61"W	
Santa Lucía	1	28.9	MHNM 1189	Uruguay	Canelones, Rio Santa Lucía basin, Canelón Grande stream	34°29'14.70"S, 56°20'34.54"W	
Pando	2	33.6–33.9	MHNM 812	Uruguay	Canelones, Cañada de Ramos, Pando, Pando stream	34°43'39.01"S, 55°56'39"W	
Pando	1	30.6	MLP 14443	Uruguay	Canelones, Cañada de Ramos, Pando, Pando stream	34°44'19.2"S, 55°56'27"W	
Pando	3	22.2–25.3	MLP 11444*	Uruguay	Canelones, Cañada de Ramos, Pando, Pando stream	34°42'12"S, 55°56'42.6"W	
Pando	10	25.3–34.8	MLP 11445	Uruguay	Canelones, Cañada de Ramos, Pando, Pando stream	34°44'19.2"S, 55°56'27"W	1 c&s: 28.7 mm SL
Pando	1	25.2	UNMDP 5219**	Uruguay	Canelones, Cañada de Ramos, Pando, Pando stream	34°42'12"S, 55°56'42.6"W	
Middle Negro	28	19.6–29.8	MHNM 4018	Uruguay	Durazno, marginal lagoon to Río Yi, Estancias del Lago	33°21'47.16"S, 56°35'23.43"W	15 fully measured
Upper Negro	10	25.9–33.6	UFRGS 8119	Uruguay	Cerro Largo, small stream at Route 26, ca. 59 km from Melo, between Sauce creek and Fraile Muerto creek	32°17'39"S, 54°44'59"W	
Upper Negro	2	27.4–28.7	UFRGS 8120	Uruguay	Tacuarembó, Rio Tacuarembó, at Route 26, Villa Ansina	31°58'33"S, 55°28'13"W	
Upper Negro	1	24.3	UFRGS 8121	Uruguay	Rivera, Mazangano Bridge at Route 44	32°06'33"S, 54°40'08.6"W	
Upper Negro	11	27.2–32.0	UFRGS 8122	Uruguay	Rivera, lateral puddles and Corrales creek, affluent of Rio Tacuarembó, Route 27	31°23'26"S, 55°15'14"W	3 c&s: 30.4–31.5 mm SL
Upper Negro	5	27.3–29.1	UFRGS 8123	Uruguay	Tacuarembó, Caraguatá creek, tributary to Rio Tacuarembó, Route 26, Las Toscas	32°09'29"S, 55°01'27"W	
Upper Negro	1	25.1	UFRGS 8429	Brazil	Rio Grande do Sul, Bagé, road between Aceguá and Bagé, Rio Negro	31°28'37"S, 54°08'20"W	
Upper Negro	10	25.9–33.6	UFRGS 8464	Brazil	Rio Grande do Sul, Bagé, road between Aceguá and Bagé, BR-153, Cinco Saltos creek, affluent of Rio Negro	31°36'53"S, 54°08'42"W	
Upper Negro	1	29.6	UFRGS 28705	Brazil	Rio Grande do Sul, Bagé, road between Aceguá and Bagé, BR-153, Cinco Saltos creek, affluent of Rio Negro	31°36'53"S, 54°08'42"W	holotype

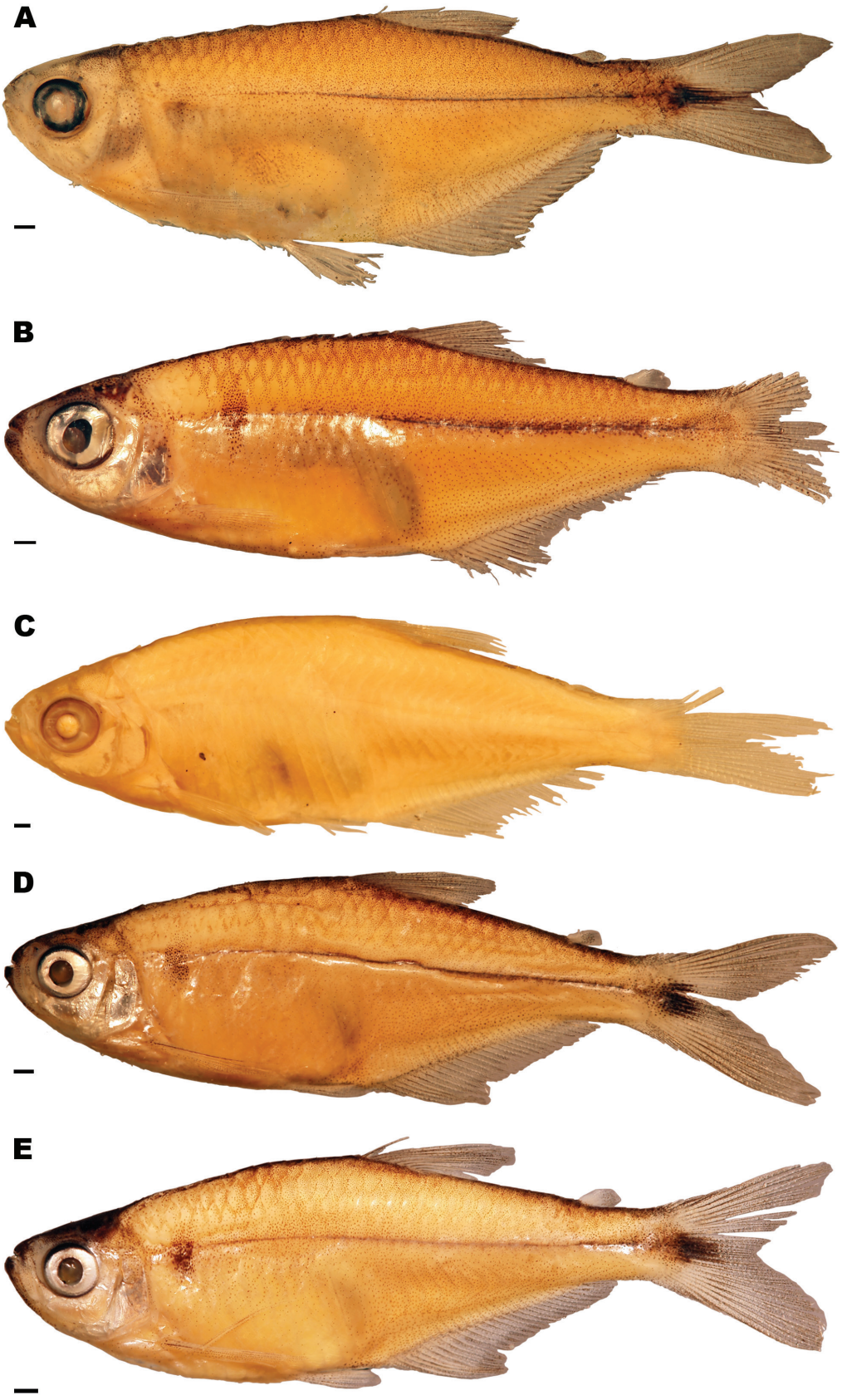

Figure 2. Extern morphology of studied specimens of *Diapoma pampeana*. **A.** MLP 11443, male, 30.6 mm SL, Uruguay, Pando Stream; **B.** MLP 11445, female, 35.1 mm SL, Uruguay, Pando Stream; **C.** MHNM 1125, female, 31.3 mm SL, Uruguay, Canelón Grande Stream; **D.** MHNM 4018, male, 29.8 mm SL, Uruguay, marginal lagoon to Rio Yi; **E.** MHNM 4018, female, 29.3 mm SL, Uruguay, marginal lagoon to Rio Yi. Photographs of the specimens from the Upper Negro are available in Ito *et al*. (2022). Scale bar: 1 mm.

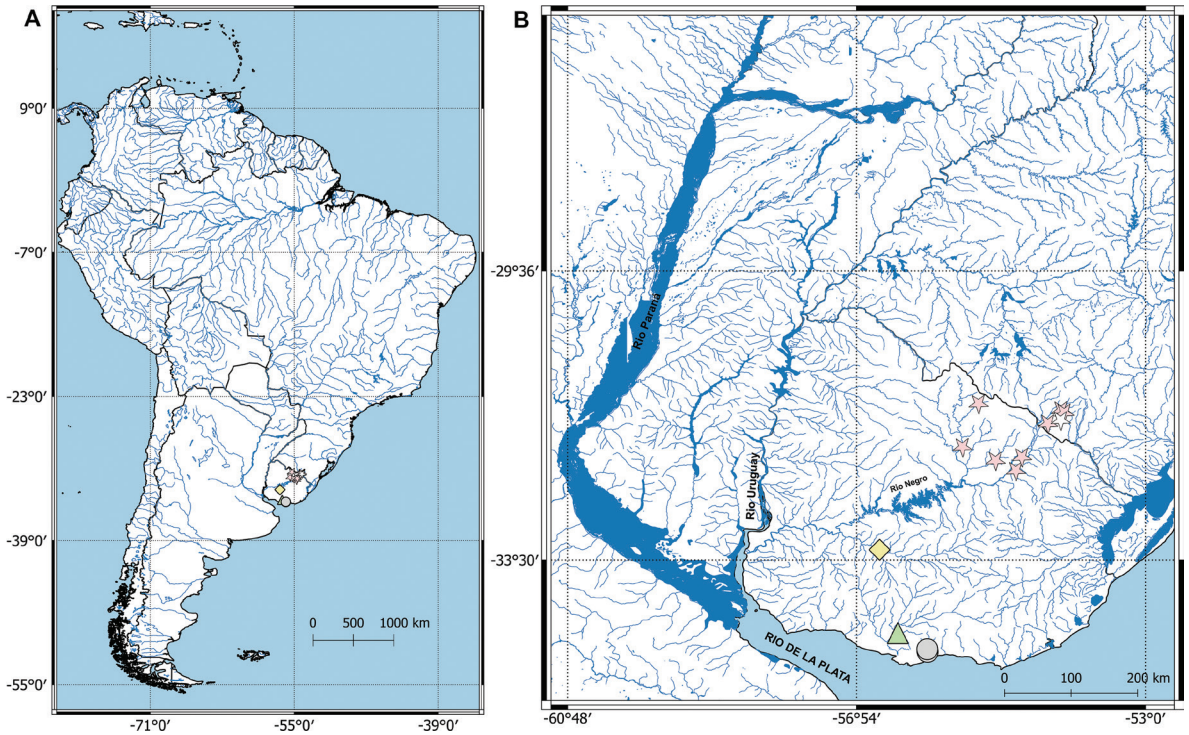

Figure 3. Geographic distribution of *Diapoma pampeana*. **A.** View within South America; **B.** View within Brazil and Uruguay. All studied specimens from the Pando (Circle), Santa Lucía (triangle), Yi (diamond), and Upper Negro (star; holotype represented by not-filled pattern) are depicted. Other records presented by Ito et al. (2022) are also included.

Table 2. Comparative morphometric data obtained in the specimens studied of *D. pampeana*. SD = standard deviation; n = number of examined specimens; CI = confidence interval. Group names corresponds with those described in the text.

	Pando (n = 17)			Santa Lucía (n = 2)			Middle Negro (n = 15)			Upper Negro (n = 35)		
	Range	Mean±SD	CI95%	Range	Mean±SD	CI95%	Range	Mean±SD	CI95%	Range	Mean±SD	CI95%
Standard Length (mm)	22.2–35.1	28.9±3.8	27.1; 30.6	28.9–31.3	30.1±1.7	28.9; 31.3	23.3–29.8	26.6±1.7	25.8; 27.4	25.1–33.6	29.4±2.2	28.7; 30.1
Percents of SL (%)												
Depth at dorsal-fin origin	29.5–34.7	31.7±1.4	31.1; 32.4	30.1–32.2	31.1±1.5	30.1; 32.2	29.6–33.4	31.5±1.3	30.9; 32.1	27.7–33.7	30.9±1.2	30.5; 31.3
Snout to dorsal-fin origin	53.5–58.2	55.7±1.4	55.1; 56.4	54.2–55.7	54.9±1.1	54.2; 55.7	54.2–57.6	55.8±1.0	55.4; 56.3	49.0–56.2	52.7±1.7	52.3; 53.3
Snout to pectoral-fin origin	24.7–27.3	26.2±0.9	25.8; 26.6	25.2–26.2	25.7±0.7	25.2; 26.2	25–28.3	26.4±0.8	26.0; 26.8	23.2–27.5	25.1±0.9	24.8; 25.4
Snout to pelvic-fin origin	44.1–47.8	46.5±1.0	46.1; 47.0	44.7–45.0	44.9±0.2	44.7; 45.0	44.3–48.2	45.8±1.0	45.3; 46.3	41.9–47	44.9±1.2	44.5; 45.3
Snout to anal-fin origin	56.6–62.1	59.9±1.5	59.3; 60.7	57.9–58.5	58.2±0.4	57.9; 58.5	56.6–60.6	58.7±1.2	58.2; 59.3	53.8–60.6	58.3±1.5	57.8; 58.8
Distance between dorsal- and adipose-fin origins	30.4–34.8	33.0±1.1	32.5; 33.5	33.6–34.4	34.0±0.6	33.6; 34.4	32.0–36.1	33.9±1.0	33.4; 34.4	33.0–39.9	37.1±1.4	36.6; 37.5
Dorsal fin to caudal-fin base	46.4–49.0	47.7±0.9	47.3; 48.1	45.5–48.6	47.1±2.2	45.5; 48.6	46.1–49.7	48.2±1.3	47.6; 48.9	45.9–54.8	49.0±1.9	48.2; 49.3
Dorsal-fin length	20.7–24.8	23.0±0.9	22.6; 23.5	23.2–24.0	23.6±0.6	23.2; 24.0	22.7–25.1	23.9±0.7	23.6; 24.3	22.7–27.0	24.6±1.2	24.2; 25.0
Dorsal-fin base length	9.7–12.8	11.1±0.7	10.7; 11.4	10.4–12.2	11.3±1.3	10.4; 12.2	10.5–11.9	11.0±0.4	10.8; 11.3	10.1–14.0	11.7±0.9	11.4; 12.0
Pectoral-fin length	21.6–25.0	23.1±1.0	22.6; 23.6	22.2–23.2	22.7±0.7	22.2; 23.2	20.9–24.4	22.6±0.9	22.2; 23.1	21.9–25.8	23.8±0.9	23.5; 24.1
Pelvic-fin length	11.1–14.7	13±0.9	12.5; 13.4	12.2–12.3	12.2±0.1	12.2; 12.3	11.2–13.7	12.6±0.8	12.2; 13.0	12.0–15.7	13.9±0.9	13.5; 14.2
Anal-fin base length	30.2–37.0	33.5±1.8	32.7; 34.3	31.4–35.1	33.3±2.6	31.4; 35.1	31.7–34.3	33.0±0.9	32.5; 33.4	32.1–36.6	34.5±1.3	34.0; 34.9
Caudal peduncle depth	8.6–11.6	10.1±0.7	9.8; 10.4	10.5–10.7	10.6±0.2	10.5; 10.7	9.6–11.0	10.4±0.4	10.2; 10.7	7.8–10.0	9.0±0.5	8.8; 9.2
Caudal peduncle length	12.1–14.6	13.6±0.7	13.3; 13.9	12.1–13.4	12.8±0.9	12.1; 13.4	12.5–15.0	13.4±0.6	13.1; 13.7	8.9–13.4	11.3±1.0	11.0; 11.6
Head length	21.9–25.4	23.7±0.9	23.3; 24.1	21.7–22.9	22.3±0.9	21.7; 22.9	22.5–25.3	23.5±0.8	23.1; 23.9	21.3–25.2	23.1±0.9	22.8; 23.3
Percents of HL (%)												
Snout length	19.3–22.3	21.0±0.8	20.7; 21.4	21.5–21.6	21.5±0.1	21.5; 21.6	20.1–22.1	20.8±0.6	20.5; 21.1	16.3–22.1	19.1±1.6	18.6; 19.7
Horizontal eye length	38.8–45.0	42.1±1.6	41.4; 42.9	41.8–42.8	42.3±0.7	41.8; 42.8	40.2–44.5	42.3±1.3	41.7; 42.9	39.5–46.8	43.5±1.6	43.0; 44.1
Postorbital head length	36.7–42.8	39.2±2.1	38.2; 40.1	38.3–40.2	39.3±1.3	38.3; 40.2	35.4–40.0	38.0±1.3	37.3; 38.6	35.6–43.1	39.2±1.9	38.5; 39.8
Least interorbital width	30.1–36.0	33.3±1.8	32.5; 34.1	34.2–34.9	34.5±0.5	34.2; 34.9	28.8–35.9	33.4±1.8	32.6; 34.3	28.6–38.7	32.2±1.9	31.6; 32.8
Upper jaw length	32.8–44.5	36.5±2.9	35.1; 37.8	39.1–39.9	39.5±0.6	39.1; 39.9	32.7–37.1	35.3±1.4	34.7; 36.1	32.4–39.1	35.7±1.8	35.1; 36.3
Dentary length	37.1–46.4	40.3±2.4	39.1; 41.3	39.1–39.8	39.4±0.5	39.1; 39.8	37.7–42.8	40.3±1.6	39.5; 41.0	36.5–42.2	38.9±1.6	38.3; 39.4

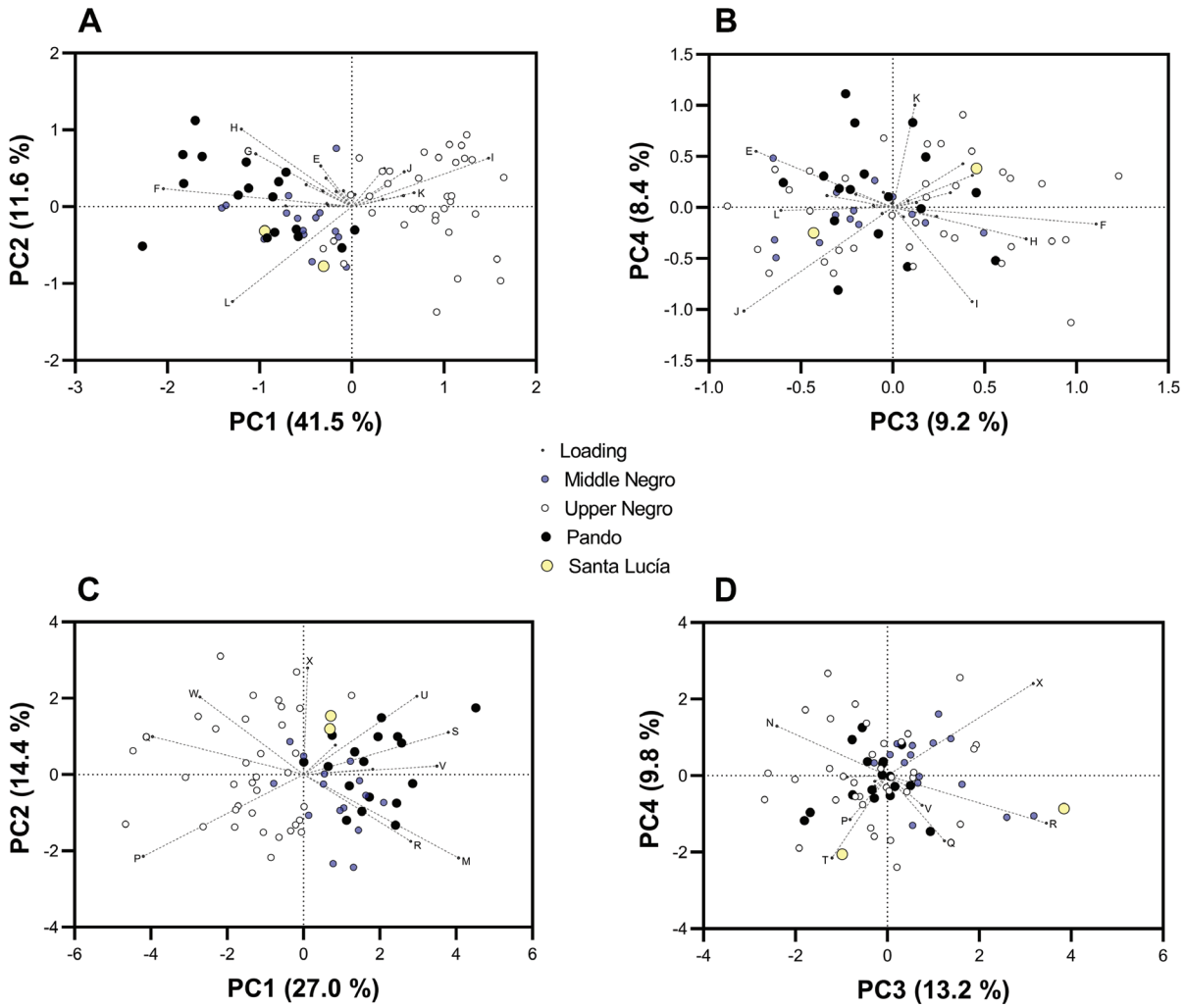

Figure 4. Most discriminant axes obtained from the PCA analyses performed using morphometric and meristic data of studied specimens of *Diapoma pampeana* (in each plot, the loadings are scaled to 90% of the PC scores). Size-corrected measurements: **A.** PC1 *vs.* PC2 plot; **B.** PC3 *vs*. PC4 plot. Meristic data; **C.** PC1 *vs.* PC2 plot; **D.** PC3 vs. PC4 plot. Only these variables that most loaded the components are indicated as follows: E- depth at dorsal-fin origin; F- snout to dorsal-fin origin; G- snout to pelvic-fin origin; H- Snout to anal-fin origin; I- distance between dorsal- and adipose-fin origins; J- dorsal fin to caudal-fin base; K- anal-fin base length; L- caudal peduncle length; M- longitudinal scales; N- lateral-line scales; P- scales between lateral line-dorsal origin; Q- scales between lateral line-pelvic origin; R- circumpeduncular scales; S- predorsal scales; T- number of branched anal-fin rays; U- gill rakers on upper limb of branchial arch; V- gill rakers on lower limb of branchial arch; W- number of maxillary teeth; X- number of dentary teeth.

as the snout to anal-fin origin (0.3), depth at dorsal-fin origin (0.2), snout to pelvic-fin origin (0.2), and distance between the dorsal- and adipose-fin origins (0.2). PC3 was most affected by the dorsal fin to caudal-fin base (-0.3), whereas PC4 was most strongly loaded by the anal-fin base (0.3).

The cluster analysis showed that the four groups analyzed were distributed into two large clusters (most bootstrap values were below 50). All the specimens of the Upper Negro group (except three) were almost completely separated from the Pando, Santa Lucía, and Middle Negro groups. In contrast, the specimens of the Pando group were not clustered separately, but were instead mixed mainly with the specimens of the Santa Lucía and Middle Negro groups (Suppl. material 4).

The comparative results obtained in the meristic data are presented in Table 4. The first four components (explained 64.4% of the total variance, Suppl. material 3) were chosen as significant to analyze the variation in the meristic data, following the same criteria used for the morphometric data (Fig. 4C, D; Suppl. material 2). The Pando group was slightly differentiated from the Upper Negro group along the horizontal axis in the PC1 vs. PC2 plot (accounted for 41.3% of the total variance, Fig. 4C), but overlapped almost completely with the other groups. In the PC3 vs. PC4 plot (explained 23.0% of the total variance, Fig. 4D), the Pando group was not separately distributed from the other groups along the axes. PC1 was most strongly influenced by the number of longitudinal scales (0.7) and predorsal scales (0.7) (Fig. 4C, Table 3). PC2 was strongly loaded by the number of dentary (0.7) and maxillary (0.5) teeth, and number of gill rakers on the upper limb of the first branchial arch (0.5) (Table 3). PC3 was mainly influenced by the number of pored lateral-line scales (-0.7), whereas PC4 was greatly affected by the number of branched anal-fin rays (-0.7). Tukey

Table 3. Loadings obtained from the PCA analyses using morphometric and meristic data. Percentages of variance are reported.

Variables	Components			
	1	2	3	4
Morphometric data:	41.5%	11.6%	9.2%	8.4%
Depth at dorsal-fin origin	-0.1	0.2	-0.2	0.2
Snout to dorsal-fin origin	-0.5	0.1	0.1	0.0
Snout to pectoral-fin origin	-0.1	0.1	0.0	0.0
Snout to pelvic-fin origin	-0.2	0.2	0.0	0.0
Snout to anal-fin origin	-0.3	0.3	0.1	-0.1
Distance between dorsal- and adipose-fin origins	0.5	0.2	0.1	-0.2
Dorsal fin to caudal-fin base	0.2	0.1	-0.3	-0.2
Dorsal-fin length	0.2	0.0	0.1	0.1
Dorsal-fin base length	0.1	0.0	-0.1	0.0
Pectoral-fin length	0.1	0.1	0.0	0.0
Pelvic-fin length	0.1	0.1	0.1	0.1
Anal-fin base length	0.2	0.1	0.0	0.3
Caudal peduncle depth	-0.2	0.0	-0.1	0.0
Caudal peduncle length	-0.3	0.0	-0.2	0.0
Head length	-0.1	0.1	0.0	0.0
Snout length	-0.1	0.0	0.0	0.0
Horizontal eye length	0.0	0.0	0.0	0.0
Postorbital head length	0.0	0.1	0.0	0.0
Least interorbital width	-0.1	0.0	0.0	0.0
Upper jaw length	0.0	0.1	0.0	0.0
Lower jaw length	-0.1	0.1	0.0	0.0
Meristic data:	27.0%	14.4%	13.2%	9.8%
Longitudinal scales	0.7	-0.4	0.1	-0.1
Lateral-line scales	0.3	0.0	-0.7	0.0
Scales between lateral line-dorsal origin	-0.6	-0.4	-0.2	-0.4
Scales between lateral line-pelvic origin	-0.6	0.2	0.2	-0.5
Circumpeduncular scales	0.5	-0.3	0.6	-0.4
Predorsal scales	0.7	0.3	-0.1	0.0
Branched anal-fin rays	0.2	0.2	-0.4	-0.7
Gill rakers upper limb of branchial arch	0.5	0.5	-0.3	0.0
Gill rakers lower limb of branchial arch	0.6	0.1	0.1	-0.2
Maxillary teeth	-0.4	0.5	-0.1	-0.1
Dentary teeth	0.0	0.7	0.5	0.1

box plots of counts that most affected PCA and were most distinctive for the Pando group are presented in Suppl. material 5. The multivariate analyses performed on the morphometric and meristic data converged in coincident results that, despite having overlap between some individuals, showed the population from the Pando stream to be somewhat distinctive morphologically from the specimens from the upper Rio Negro basin. The number of vertebrae of the Pando group was observed within the range of variation of the Upper Negro group (34 vs. 34–35).

The pigmentation pattern observed in the Pando group (Figs 1, 2A, B) was similar to that found in the Upper Negro groups (Ito et al. 2022: figs 1–3), mainly characterized by the vertically enlarged humeral spot, the narrow and conspicuous black line along the horizontal septum of body (in some specimens of the Pando group, it was observed to be somewhat silvery), the longitudinal black stripe extending posteriorly on the middle caudal-fin rays, and the presence of a small black blotch, restricted to the base of the middle caudal-fin rays. The specimens of the Middle Negro group (Fig. 2D, E) were observed to be similarly pigmented as the other groups, except for the caudal-fin blotch, which was not completely extended along the middle rays in some specimens. The examined specimens of the Santa Lucía group were found slightly faded (Fig. 2C), but some pigmentation characters of *D. pampeana* as those aforementioned were found to be present.

Molecular comparisons

The genetic variation seen, based on the Tajima-Nei distance between the Pando specimens and the specimens from the upper Negro basin of *D. pampeana* were found to be very low or nearly zero (≤ 0.002), even when bootstrapped (10000). In the NJ topology (Fig. 5), the two specimens of the Pando stream analyzed were placed together with the remaining specimens of *D. pampeana* from the upper Negro basin and, particularly, as closely related to one specimen of that basin than between each other (Fig. 5). The Bayesian topology showed that *D. pampeana* was more related to *D. guarani* and *D. obi* within a common clade with *D. potamohadros* and *D. tipiaia* (Fig. 6). In both the Bayesian and NJ trees, the analyzed specimens of *Diapoma* from the Pando stream were strongly placed together in the same clade with the specimens of *D. pampeana*. The general pattern of interrelationships among the *Diapoma* species was found to be almost similar between both methods. The uncorrected pairwise mean distance obtained for *D. pampeana* ranged from 3.5 to 7.6% (Suppl. material 6: the lowest value with *D. obi* and the highest value with *D. itaimbe*). The intraspecific variation of *D. pampeana* was observed to be varying from 0 to 0.2%. Only one specimen of the Upper Negro group (UFRGS

Table 4. Comparative meristic data obtained for the studied specimens of *D. pampeana*. SD = standard deviation; n = number of examined specimens. Mean and mode values are reported. Group names corresponds with those described in the text.

	Pando			Santa Lucía			Middle Negro			Upper Negro		
	Range	Mean/ Mode±SD	n	Range	Mean/ Mode±SD	n	Range	Mean/ Mode±SD	n	Range	Mean/ Mode±SD	n
Longitudinal scales	35–38	36.9/37±0.9	17	35–37	36.0/N/A±1.4	2	35–39	37.0/36±1.1	15	32–37	35.1/36±1.2	35
Lateral-line scales	7–9	7.8/7±0.8	17	5–8	6.5/N/A±2.1	2	5–8	6.7/7±1.0	15	5–9	7.3/8±1.0	35
Scales between lateral line-dorsal origin	5–5	5.0/5±0.0	17	5–5	5.0/N/A±0.0	2	5–5	5.0/5±0.0	15	5–6	5.6/6±0.5	35
Scales between lateral line-pelvic origin	4–5	4.1/4±0.2	17	5–5	5.0/N/A±0.0	2	4–5	4.1/4±0.4	15	4–5	4.5/4±0.5	34
Circumpeduncular scales	14–15	14.1/14±0.3	15	15	N/A	1	14–15	14.3/14±0.5	15	11–15	13.0/13±0.9	35
Predorsal scales	12–15	13.6/13±0.8	17	14–15	14.5/N/A±0.7	2	11–13	12.3/12±0.6	15	10–14	12.3/12±0.8	35
Branched anal-fin rays	21–26	23.4/23±1.4	17	22–26	24.0/N/A±2.8	2	21–25	22.8/23±1.1	15	21–25	22.8/22±1.1	35
Gill rakers upper limb of branchial arch	7–10	8.3/8±0.8	14	7	N/A	1	7–8	7.5/7±0.5	15	6–9	7.1/7±0.9	34
Gill rakers lower limb of branchial arch	14–18	14.9/14±1.2	14	15	N/A	1	14–15	14.3/14±0.5	15	13–15	13.9/14±0.8	35
Maxillary teeth	1–3	1.6/2±0.6	15	2	N/A	1	1–2	1.3/1±0.5	15	1–4	2.1/3±0.9	34
Dentary teeth	7–11	8.8/9±1.1	15	12	N/A	1	7–11	9.0/9±1.0	15	6–14	9.0/9±1.3	35

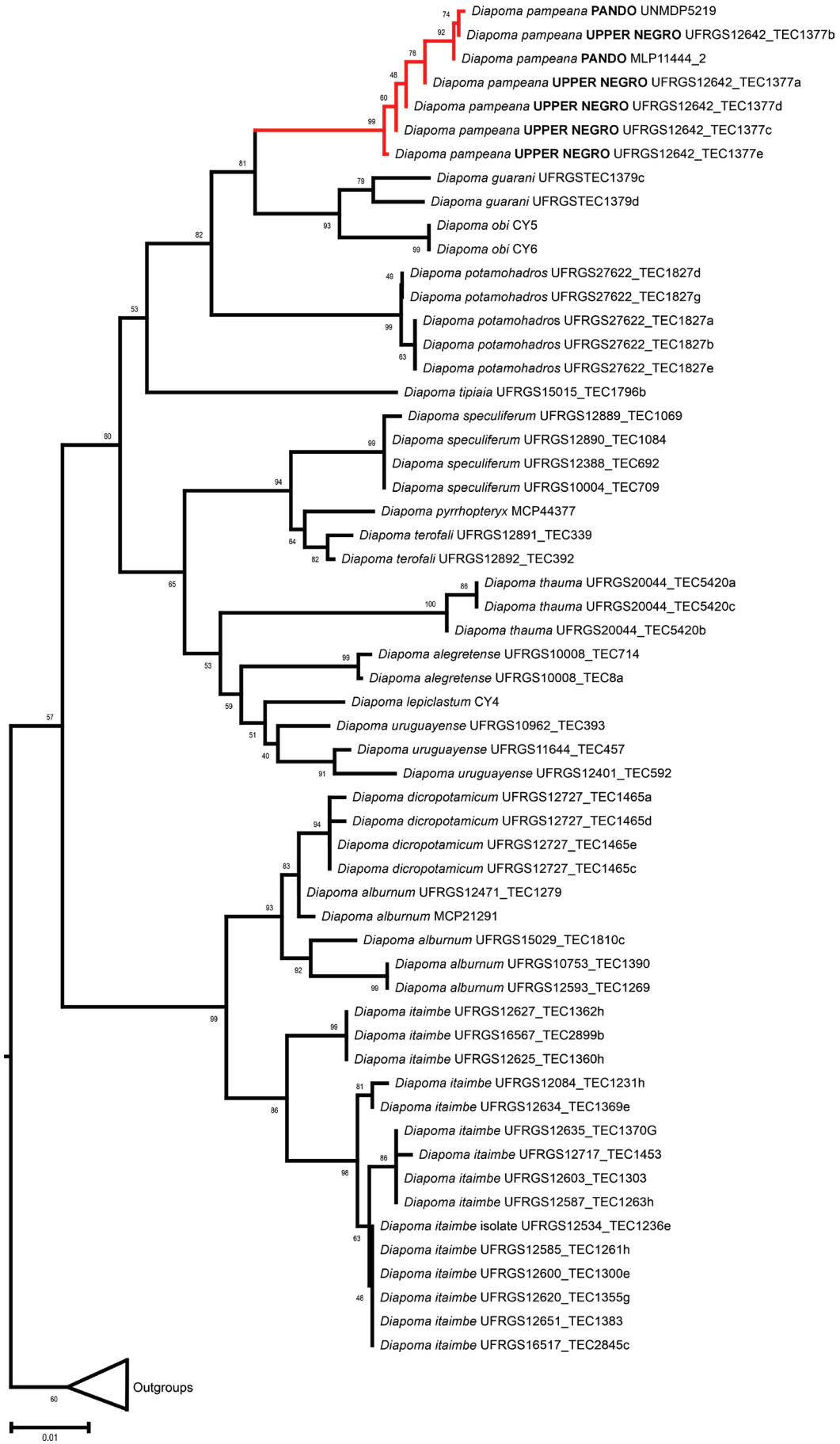

Figure 5. Neighbor-Joining topology of analyzed *Diapoma* specimens based on Tamura-Nei model and COI sequence data. Bootstrap values (10000 replicates) are shown below the branches. SBL = 0.783.

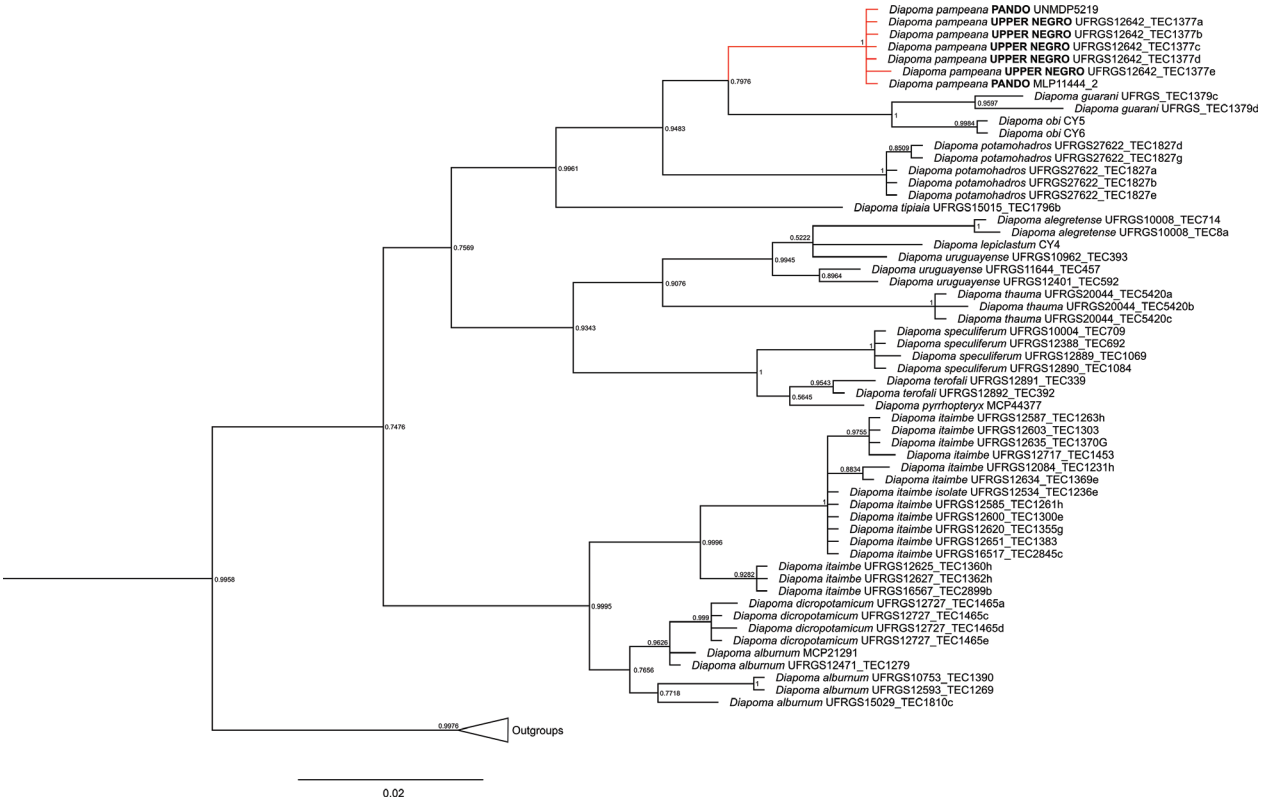

Figure 6. Bayesian topology of phylogenetic relationships among the analyzed *Diapoma* species (comparing specimens of *D. pampeana* from the Pando stream and Upper Negro basin) based on COI sequence data. Numbers at nodes correspond to posterior probabilities.

12642: TEC1377e) showed the greater p-distance (0.2%) in each comparison with the other specimens analyzed of *D. pampeana* (Suppl. material 6).

In the polymorphism analysis comparing the Pando and Upper Negro specimens, 728 sites were analyzed (381: invariable; 347: with gaps or missing data), resulting in one polymorphic site (singleton) and two haplotypes (Hd = 0.286; variance = 0.034; standard deviation = 0.196). In general, the nucleotide diversity was extremely low (π = 0.00095; θ = 0.00107; k = 0.286) for the samples analyzed. No variation was found within the Pando samples (π = 0.00000; k = 0.000). For the Upper Negro samples, only one polymorphic site (monomorphic in the Pando samples) was found and, thus, their diversity was slightly greater (π = 0.00105; k = 0.400). There were no observed shared mutations between these two populations. Regarding the divergence between the populations compared, the values obtained were low (Dxy = 0.00052; Da = 0.00000). The haplotype network showed a simple structure of two groups without well-defined geographic structure and in which one of them was mixed (Suppl. material 7).

Comparative examined material

Diapoma alburnum: UFRGS 13309, 11, 33.4–56.0 mm SL. *Diapoma guarani*: MHNG 2366.99, holotype, 31.7 mm SL. *Diapoma lepiclastum*: MACN-ict 9682, 47, 29.3–42.0 mm SL. *Diapoma obi*: MLP 11312, 3, 29.5–35.6 mm SL. MACN-ict 9560, holotype, 52.6 mm SL. *Diapoma uruguayense*, MACN-ict 9681, 7, 31.6–34.6 mm SL.

Discussion

The stevardiine species *D. pampeana* was recently described from several localities along the Rio Negro basin in Brazil and Uruguay (Ito et al. 2022). The freshwater fish fauna from the Pando stream is mainly known from studies focused on estuarine-influenced coastal waters (Plavan et al. 2010; Gurdek and Acuña-Plavan 2017). Although the body coloration was similar between the specimens of the Pando and Upper Negro groups, the former showed a striking morphometric and meristic divergence from the latter. Additionally, the intraspecific variation between the Pando and Upper Negro populations became much more subtle when compared with specimens from geographically intermediate areas such as the Santa Lucía and Middle Negro basins (*i.e.* the specimens of these groups were slightly more similar to each other in the morphometric and meristic data than to the specimens of the Upper Negro). Frequently, in morphological comparisons using multivariate methods, the populations exhibiting major differences in body shape correspond with those morphotypes that are located at the farthest distance geographically from the others (Lazzarotto et al. 2017; Vanegas-Rios et al. 2019; Rodrigues-Oliveira et al. 2023). In consequence, the analyzed specimens of *D. pampeana* may be responding to a gradual pattern of divergence associated with spatial segregation, often observed in widespread species (Lazzarotto et al. 2017; Arroyave et al. 2019; Vanegas-Rios et al. 2019; Rodrigues-Oliveira et al. 2023).

In the morphological comparisons performed herein, the Pando group was greatly differentiated in the size-corrected PCA from the Upper Negro group along PC1, which was mainly influenced by the following distances: snout to dorsal-fin origin, snout to anal-fin origin, dorsal- and adipose-fin origins, and caudal peduncle length (Fig. 4A). Some measurements such as the snout to dorsal-fin origin, snout to anal-fin origin, snout to pelvic-fin origin, distance between the dorsal- and pectoral-fin origins, head length, snout length, and eye diameter have been found to be taxonomically informative to discriminate among *Diapoma* species (Malabarba and Weitzman 2003; Vanegas-Ríos et al. 2018; Ito et al. 2022). Based on the meristic data, these groups were also found to be slightly divergent from each other along PC1. For this component, some main counts defining the variability were the number of longitudinal scales and predorsal scales (Table 3, Fig. 4C). Usually, the range is used as the main indicator to define the limits of the morphological variation among species in measurements or counts (Garavello et al. 1992; Aguirre et al. 2016; Lazzarotto et al. 2017; Arroyave et al. 2019; Vanegas-Rios et al. 2019; Malabarba et al. 2021). The main dilemma for defining these limits appears when data have varied degrees of overlapping between populations of study.

Further statistical procedures are used as a complement to test if diverging tendencies in morphometric data are, or are not, significant (Lazzarotto et al. 2017; Arroyave et al. 2019; Vanegas-Rios et al. 2019; Rodrigues-Oliveira et al. 2023). For instance, it is frequently found that subtle or moderate intraspecific differences in body shape result in being statistically significant, but it may be also associated with the degree of sensitivity involved in pairwise tests (e.g. means). Recently, the statistical potential behind morphometrically divergent patterns has been used to propose subspecies within gymnotids (Craig et al. 2017). Such criterion is not commonly used in modern ichthyology, so that the erection of infraspecific categories can be considered unnecessary to understand the intraspecific variation (e.g. clines) (Kottelat 1998; Kullander 1999). In the case of the Pando group, it seems unjustified to propose a new infraspecific category under the light of the current evidence described from morphological data, even more when it is geographically isolated and its phenotypic variation is described and contextualized in the present contribution. In a similar case, geographically isolated coastal river populations of *D. itaimbe* that showed a statistically significant difference in overlapping ranges of anal-fin ray counts were treated as structured isolated populations instead of separate species (Malabarba and Weitzman 2003; Hirschmann et al. 2015).

When the discriminative tendencies are striking, as occurred here between the Pando and Upper Negro groups, including additional independent evidence, such as DNA data, can help to support the conclusion. The COI marker has played an important role in resolving taxonomic questions in freshwater fishes (Pereira et al. 2013). In general, comparative studies using COI and morphology are dealing with cryptic species, species complexes or populations with slight morphological variations (under a context of geographic isolation) (Serrano et al. 2019; Garavello et al. 2021; Guimarães et al. 2021; Malabarba et al. 2021; Aguilera et al. 2022). The phylogenetic signal of the COI marker within *Diapoma* has been studied and used to propose intraspecific and interspecific limits, as well as new species (Casciotta et al. 2012; Hirschmann et al. 2015; Ito et al. 2022). However, the use of this marker by itself for recognizing species (e.g. as single locus without morphological or cytogenetic support) has its own methodological limits, and it is especially important to have this into account when dealing with complex groups of species or populations (Castro Paz et al. 2014; García-Melo et al. 2019; Klimov et al. 2019; Silva-Santos et al. 2023). This may imply that in some cases there is no guarantee of complete interspecific delimitation (e.g. Castro Paz et al. 2014).

The phylogenetic comparison performed using the COI marker of all known species of *Diapoma* (except *D. nandi* from the Paraná basin) recovered the Pando group as part of *D. pampeana*. It also demonstrates that the recognition of the Pando group as separate would make *D. pampeana* paraphyletic (Fig. 5: NJ topology). The variability of the p-distances calculated for the Pando group were observed to be lower than the average congeneric values (0–0.2% vs. 1.3–8.0%), as it has been often reported in other characids (Pereira et al. 2011b; García-Melo et al. 2019; Silva-Santos et al. 2023). Furthermore, the mean genetic distances were 3.5% and 4.3% between *D. pampeana* and its closest related species (*D. obi* and *D. guarani*, respectively). The intraspecific values obtained for *D. pampeana* are within the conspecific variation reported in species of other characid groups such as *Astyanax* (from the Rio Paraguaçu basin, mean = 0–1.7%); *Hyphessobrycon* Durbin, 1908 (from the Amazon basin, mean = 0–8.9%), and some stevardiines (*Bryconamericus*, *Eretmobrycon* Fink, 1976, *Hemibrycon* Günther, 1864, *Knodus* Eigenmann, 1911, and *Piabina*: 0–1.9%) (Pereira et al. 2011b; Castro Paz et al. 2014; García-Melo et al. 2019; Silva-Santos et al. 2023). In barcoding studies, 2% threshold limit (at least 10 times the average conspecific values) has been used as the cutoff divergence value for delimiting species or molecular operational taxonomic units (Hebert et al. 2004; Ward 2009). However, an alternative threshold value of 1% has been considered for studying species complexes (Hubert et al. 2008; Pereira et al. 2011a; Silva-Santos et al. 2023). Therefore, these threshold values should be cautiously evaluated for each case in particular.

The results obtained from the exploratory analysis using haplotype, allowed us to detect the potential presence of two haplotypes that were separated by a single mutational change. Additionally, the Pando group presented the same haplotype as the Upper Negro group, which again reinforces the great resemblance between both groups. Additionally, no well-defined lineages were detected in the molecular comparisons. However, this needs to be further investigated so that within *Diapoma*, for instance, it has been found that *D. itaimbe* forms populations with well-defined structural lineages associated with a coastal biographic pattern (Hirschmann et al. 2015). The recognition of species as

separately evolving metapopulation lineages is a unifying concept in defining species (De Queiroz 2007), and so far, we have no support from molecular data to separate the Pando group from *D. pampeana*.

Freshwater fishes have limited their ability to disperse across brackish, marine or terrestrial barriers, being biologically restricted to water bodies after their formation, and thus, the disjunct geographic range associated with species and populations across several basins might be explained by river captures or dispersal favored by temporary connections (Albert and Reis 2011; Thomaz et al. 2017; Camelier et al. 2018; Cassemiro et al. 2023). These potential explanations would be plausible for testing in *D. pampeana* if its distribution was really widespread along most coastal drainages in Uruguay, as our findings suggest.

Conclusion

We concluded that the specimens from the Pando stream, despite the morphological divergence observed, can be classified as *D. pampeana*. We supported our decision based on the following arguments: 1) the deviations found on the morphometric and meristic data (e.g. PCA) are not enough to erect a new species and, as consequence, the intraspecific variability is increased; 2) the specimens of the Pando group were similarly pigmented as the specimens of the Upper Negro group (sharing the same diagnostic pattern on the humeral mark, midlateral stripe, and caudal-fin pigmentation); 3) the COI-based phylogenetic procedures supported the placement of the Pando group within the genetic variation of the Upper Negro group (typical distribution of *D. pampeana*); and 4) based on the genetic distances, the Pando group was found to be genetically similar to the Upper Negro group, with p-distances (0–0.2%) being lower than the mean distances obtained between each congener (1.3–8.0%). Additionally, the present work also confirmed the presence of *D. pampeana* in the Yi (Middle Negro basin) and Santa Lucía river basins, based on morphological evidence. Although it was not possible to separate species, our results provide new information that can be further appreciated. For instance, it has been proposed that diverging populations can represent separate evolutionarily significant units, which should be conserved (Moritz 1994; de J. May-Itzá et al. 2012; Stockwell et al. 2013; Berger et al. 2018). The geographic range of *D. pampeana* seems to be incompletely understood and might be more widely represented along the Rio Negro basin and other coastal drainages in Uruguay (Fig. 3, Suppl. material 8). Future studies may bring new insights into the population variation of the species and other phylogeographic patterns if more specimens and new localities are analyzed. The Pando population of *D. pampeana* constitutes a remarkable example of an isolated population that is morphologically divergent (in the morphometric and meristic data) from the geographically most distant conspecific population (upper Rio Negro basin), but that shares a high degree of genetic resemblance with it.

Acknowledgments

We thank the following institutions and museums for their assistance and support: G. Chiaramonte (MACN-ict); Sonia Fisch-Muller and Rafael Covain (MHNG); D. Nadalin, Jorge R. Casciotta and Adriana E. Almirón (MLP); C. Lucena (MCP), Priscila M. Ito and Juliana M. Wingert (UFRGS). The authors are grateful for the financial support provided by FONCyT (BID-PICT 2019–02419 and PIBBA 0654CO to JAVR). We are indebted to Juan José Rosso, Matías Delpiane, and Juan Martín Díaz de Astarloa (IIMyC-UNMDP), and C. Bruno and G. Giovambattista (IGEVET-UNLP) for their assistance with the DNA procedures. Nicolas Tizio (Fundación Unidos por Naturaleza), J. Pfleiderer, and F. M. Frias helped with photographs. This paper benefited from valuable suggestions and comments of anonymous reviewers, W. Costa, and F. Araújo.

References

Achkar M, Domínguez A, Pesce F (2012) Cuenca del Río Santa Lucía-Uruguay. Aportes para la discusión ciudadana. Montevideo.

Acuña A, Muñoz N, Gurdek R, Machado I, Severi V (2017) Inter-estuarine and temporal patterns of the fish assemblage of subtropical subestuaries along the Río de la Plata coast (Uruguay). Brazilian Journal of Oceanography 65(2): 173–186. https://doi.org/10.1590/s1679-87592017131106502

Aguilera G, Terán GE, Mirande JM, Alonso F, Chumacero GM, Cardoso Y, Bogan S, Faustino-Fuster DR (2022) An integrative approach method reveals the presence of a previously unreported species of *Imparfinis* Eigenmann and Norris 1900 (Siluriformes: Heptapteridae) in Argentina. Journal of Fish Biology 101(5): 1248–1261. https://doi.org/10.1111/jfb.15197

Aguirre WE, Navarrete R, Malato G, Calle P, Loh MK, Vital WF, Valadez G, Vu V, Shervette VR, Granda JC (2016) Body shape variation and population genetic structure of *Rhoadsia altipinna* (Characidae: Rhoadsiinae) in southwestern Ecuador. Copeia 104(2): 554–569. https://doi.org/10.1643/CG-15-289

Albert JS, Reis RE (2011) Historical Biogeography of Neotropical Freshwater Fishes. University of California Press, California, 388 pp. https://doi.org/10.1525/9780520948501

Almirón A, Casciotta J, Říčanová S, Dragová K, Piálek L, Říčan R (2016) First record of *Diapoma pyrrhopteryx* Menezes & Weitzman, 2011 (Characiformes: Characidae) from freshwaters of Argentina. Ichthyological Contributions of Peces Criollos 40: 1–3.

Arroyave J, Martinez CM, Stiassny MLJ (2019) DNA barcoding uncovers extensive cryptic diversity in the African long-fin tetra *Bryconalestes longipinnis* (Alestidae: Characiformes). Journal of Fish Biology 95: 379–392. https://doi.org/10.1111/jfb.13987

Azpelicueta MM, Lundberg JG, Loureiro M (2008) *Pimelodus pintado* (Siluriformes: Pimelodidae), a new species of catfish from affluent rivers of Laguna Merín, Uruguay, South America. Proceedings of the Academy of Natural Sciences of Philadelphia 157(1): 149–162. https://doi.org/10.1635/0097-3157(2008)157[149:PPSPAN]2.0.CO;2

Berger C, Štambuk A, Maguire I, Weiss S, Füreder L (2018) Integrating genetics and morphometrics in species conservation–A case study on the stone crayfish, *Austropotamobius torrentium*. Limnologica 69: 28–38. https://doi.org/10.1016/j.limno.2017.11.002

Camelier P, Menezes NA, Costa-Silva GJ, Oliveira C (2018) Molecular and morphological data of the freshwater fish *Glandulocauda melanopleura* (Characiformes: Characidae) provide evidences of river captures and local differentiation in the Brazilian Atlantic Forest. PLOS ONE 13(3): e0194247. https://doi.org/10.1371/journal.pone.0194247

Cardoso AR (2010) *Bunocephalus erondinae*, a new species of banjo catfish from southern Brazil (Siluriformes: Aspredinidae). Neotropical Ichthyology 8(3): 607–613. https://doi.org/10.1590/S1679-62252010000300005

Casciotta J, Almirón A, Piálek L, Říčan O (2012) *Cyanocharax obi*, a new species (Characiformes: Characidae) and the first record of the genus from tributaries of the río Paraná basin, Argentina. Zootaxa 3391(1): 39–51. https://doi.org/10.11646/zootaxa.3391.1.3

Cassemiro FAS, Albert JS, Antonelli A, Menegotto A, Wüest RO, Cerezer F, Coelho MTP, Reis RE, Tan M, Tagliacollo V, Bailly D, da Silva VFB, Frota A, da Graça WJ, Ré R, Ramos T, Oliveira AG, Dias MS, Colwell RK, Rangel TF, Graham CH (2023) Landscape dynamics and diversification of the megadiverse South American freshwater fish fauna. Proceedings of the National Academy of Sciences of the United States of America 120(2): e2211974120. https://doi.org/10.1073/pnas.2211974120

Castro Paz FP, Batista Jd S, Porto JIR (2014) DNA Barcodes of Rosy Tetras and Allied Species (Characiformes: Characidae: *Hyphessobrycon*) from the Brazilian Amazon Basin. PLOS ONE 9(5): e98603. https://doi.org/10.1371/journal.pone.0098603

Cattel R (1966) The scree test for the number of factors. Multivariate Behavioral Research 1: 245–276. https://doi.org/10.1207/s15327906mbr0102_10

Craig JM, Crampton WGR, Albert JS (2017) Revision of the polytypic electric fish *Gymnotus carapo* (Gymnotiformes, Teleostei), with descriptions of seven subspecies. Zootaxa 4318(3): 401–438. https://doi.org/10.11646/zootaxa.4318.3.1

Darriba D, Posada D, Kozlov AM, Stamatakis A, Morel B, Flouri T (2019) ModelTest-NG: A new and scalable tool for the selection of DNA and protein evolutionary models. Molecular Biology and Evolution 37(1): 291–294. https://doi.org/10.1093/molbev/msz189

May-Itzá W de J, Quezada-Euán JJG, Ayala R, De La Rúa P ((2012) Morphometric and genetic analyses differentiate Mesoamerican populations of the endangered stingless bee *Melipona beecheii* (Hymenoptera: Meliponidae) and support their conservation as two separate units. Journal of Insect Conservation 16: 723–731. https://doi.org/10.1007/s10841-012-9457-4

De Queiroz K (2007) Species concepts and species delimitation. Systematic Biology 56(6): 879–886. https://doi.org/10.1080/10635150701701083

Defeo O, Horta S, Carranza A, Lercari D, de Álava A, Gómez J, Martínez G, Lozoya JP, Celentano E (2009) Hacia un Manejo Ecosistémico de Pesquerías. Áreas Marinas Protegidas en Uruguay. Facultad de Ciencias-UNDECIMAR, Montevideo, 122 pp.

Dempster AP, Laird NM, Rubin DB (1977) Maximum likelihood from incomplete data via the EM algorithm. Journal of the Royal Statistical Society, Series B, Methodological 39(1): 1–38. https://doi.org/10.1111/j.2517-6161.1977.tb01600.x

Echevarría L, Gómez A, Lale M, López R, Nieto P, Pereyra G (2011) Plan de manejo costero integrado del tramo de costa A° Solís Chico –A° Solís Grande. In: Conde D (Ed) Manejo Costero Integrado en Uruguay: ocho ensayos interdisciplinarios Centro Interdisciplinario para el Manejo Costero Integrado del Cono Sur, Montevideo, 123–152.

Edgar RC (2004) MUSCLE: Multiple sequence alignment with high accuracy and high throughput. Nucleic Acids Research 32(5): 1792–1797. https://doi.org/10.1093/nar/gkh340

Elliott NG, Haskard K, Koslow JA (1995) Morphometric analysis of orange roughy (*Hoplostethus atlanticus*) off the continental slope of southern Australia. Journal of Fish Biology 46: 202–220. https://doi.org/10.1111/j.1095-8649.1995.tb05962.x

Ferreira KM, Menezes NA, Quagio-Grassioto I (2011) A new genus and two new species of Stevardiinae (Characiformes: Characidae) with a hypothesis on their relationships based on morphological and histological data. Neotropical Ichthyology 9(2): 281–298. https://doi.org/10.1590/S1679-62252011000200005

Ferreira KM, Mirande JM, Quagio-Grassiotto I, Santana JCO, Baicere-Silva CM, Menezes NA (2021) Testing the phylogenetic hypotheses of Stevardiinae Gill, 1858 in light of new phenotypic data (Teleostei: Characidae). Journal of Zoological Systematics and Evolutionary Research 59(8): 2060–2085. https://doi.org/10.1111/jzs.12517

Fink WL, Weitzman SH (1974) The so-called Cheirodontin fishes of Central America with descriptions of two new species (Pisces: Characidae) Smithsonian Contributions to Zoology 172: 1–45. https://doi.org/10.5479/si.00810282.172.

Fricke R, Eschmeyer WN, Van der Laan R (2023) Eschmeyer's Catalog of Fishes: genera, species, references. http://researcharchive.calacademy.org/research/ichthyology/catalog/fishcatmain.asp [accessed 1 December.2023]

Frontier S (1976) Etude de la dècroissance des valeurs propres dans une analyse en composantes principales: comparaison avec le modèle du bâton brisé. Journal of Experimental Marine Biology and Ecology 25: 67–75. https://doi.org/10.1016/0022-0981(76)90076-9

Garavello JC, Dos Reis SF, Strauss RE (1992) Geographic variation in *Leporinus friderici* (Bloch) (Pisces: Ostariophysi: Anostomidae) from the Paraná-Paraguay and Amazon River basins. Zoologica Scripta 21(2): 197–200. https://doi.org/10.1111/j.1463-6409.1992.tb00320.x

Garavello JC, Ramirez JL, de Oliveira AK, Britski HA, Birindelli JLO, Galetti Jr PM (2021) Integrative taxonomy reveals a new species of Neotropical headstanding fish in genus *Schizodon* (Characiformes: Anostomidae). Neotropical Ichthyology 19(4): e210016. https://doi.org/10.1590/1982-0224-2021-0016

García-Melo JE, Oliveira C, Da Costa Silva GJ, Ochoa-Orrego LE, Garcia Pereira LH, Maldonado-Ocampo JA (2019) Species delimitation of neotropical Characins (Stevardiinae): Implications for taxonomy of complex groups. PLOS ONE 14(6): e0216786. https://doi.org/10.1371/journal.pone.0216786

Guimarães KL, Rosso JJ, Souza MF, Díaz de Astarloa JM, Rodrigues LR (2021) Integrative taxonomy reveals disjunct distribution and first record of *Hoplias misionera* (Characiformes: Erythrinidae) in the Amazon River basin: morphological, DNA barcoding and cytogenetic considerations. Neotropical Ichthyology 19(2): e200110. https://doi.org/10.1590/1982-0224-2020-0110

Gurdek R, Acuña-Plavan A (2017) Temporal dynamics of a fish community in the lower portion of a tidal creek, Pando sub-estuarine system, Uruguay. Iheringia. Série Zoologia 107(0): e2017003. https://doi.org/10.1590/1678-4766e2017003

Gutiérrez JM, Villar S, Acuña Plavan A (2015) Micronucleus test in fishes as indicators of environmental quality in subestuaries of the Río de la Plata (Uruguay). Marine Pollution Bulletin 91(2): 518–523. https://doi.org/10.1016/j.marpolbul.2014.10.027

Hall TA (1999) BioEdit: A User-Friendly Biological Sequence Alignment Editor and Analysis Program for Windows 95/98/NT. Nucleic Acids Symposium Series. Oxford University Press, 95–98.

Hammer Ø, Harper DAT, Ryan PD (2001) PAST: Paleontological statistics software package for education and data analysis. Palaeontologia Electronica 4: 1–9.

Hebert PDN, Stoeckle MY, Zemlak TS, Francis CM (2004) Identification of Birds through DNA Barcodes. PLOS Biology 2(10): e312. https://doi.org/10.1371/journal.pbio.0020312

Hirschmann A, Malabarba LR, Thomaz AT, Fagundes NJR (2015) Riverine habitat specificity constrains dispersion in a Neotropical fish (Characidae) along Southern Brazilian drainages. Zoologica Scripta 44(4): 374–382. https://doi.org/10.1111/zsc.12106

Hubert N, Hanner R, Holm E, Mandrak NE, Taylor E, Burridge M, Watkinson D, Dumont P, Curry A, Bentzen P, Zhang J, April J, Bernatchez L (2008) Identifying Canadian Freshwater Fishes through DNA Barcodes. PLOS ONE 3(6): e2490. https://doi.org/10.1371/journal.pone.0002490

IBM (2019) IBM SPSS Statistics for Windows, Version 26.0. IBM Corp, Armonk, NY.

Ito PMM, Carvalho TP, Pavanelli CS, Vanegas-Ríos JA, Malabarba LR (2022) Phylogenetic relationships and description of two new species of *Diapoma* (Characidae: Stevardiinae) from the La Plata River basin. Neotropical Ichthyology 20(1): e210115. https://doi.org/10.1590/1982-0224-2021-0115

Ivanova NV, Dewaard JR, Hebert PDN (2006) An inexpensive, automation-friendly protocol for recovering high-quality DNA. Molecular Ecology Notes 6: 998–1002. https://doi.org/10.1111/j.1471-8286.2006.01428.x

Ivanova NV, Zemlak TS, Hanner RH, Hebert PDN (2007) Universal primer cocktails for fish DNA barcoding. Molecular Ecology Notes 7: 544–548. https://doi.org/10.1111/j.1471-8286.2007.01748.x

Klimov PB, Skoracki M, Bochkov AV (2019) Cox1 barcoding versus multilocus species delimitation: validation of two mite species with contrasting effective population sizes. Parasites & Vectors 12: 1–8. https://doi.org/10.1186/s13071-018-3242-5

Kottelat M (1998) Systematics, species concepts and the conservation of freshwater fish diversity in Europe. The Italian Journal of Zoology 65(sup1): 65–72. https://doi.org/10.1080/11250009809386798

Kullander SO (1999) Fish species – how and why. Reviews in Fish Biology and Fisheries 9(4): 325–352. https://doi.org/10.1023/A:1008959313491

Lazzarotto H, Barros T, Louvise J, Caramaschi EP (2017) Morphological variation among populations of *Hemigrammus coeruleus* (Characiformes: Characidae) in a Negro River tributary, Brazilian Amazon. Neotropical Ichthyology 15: e160152. https://doi.org/10.1590/1982-0224-20160152

Leigh JW, Bryant D (2015) popart: full-feature software for haplotype network construction. Methods in Ecology and Evolution 6: 1110–1116. https://doi.org/doi.org/10.1111/2041-210X.12410

Lucena CA, Malabarba LR, Reis RE (1992) Resurrection of the neotropical pimelodid catfish *Parapimelodus nigribarbis* (Boulenger), with a phylogenetic diagnosis of the genus *Parapimelodus* (Teleoastei: Siluriformes). Copeia 1992(1): 138–146. https://doi.org/10.2307/1446545

Mahnert V, Géry J (1987) Deux nouvelles espèces du genre *Hyphessobrycon* (Pisces, Ostariophysi, Characidae) du Paraguay: *H. guarani* n. sp. et *H. procerus* n. sp. Bonner Zoologische Beitrage 38: 307–314.

Malabarba LR (1983) Redescrição e discussao da posição taxonômica de *Astyanax hasemani* Eigenmann, 1914 (Teleostei, Characidae). Comunicações do Museu de Ciências da PUCRS. Serie Zoologica 14: 177–199.

Malabarba LR, Weitzman SH (2003) Description of new genus with six new species from southern Brazil, Uruguay and Argentina, with a discussion of a putative characid clade (Teleostei: Characiformes: Characidae). Comunicações do Museu de Ciências e Tecnologia da PUCRS. Série Zoologia 16: 67–151.

Malabarba LR, Chuctaya J, Hirschmann A, de Oliveira EB, Thomaz AT (2021) Hidden or unnoticed? Multiple lines of evidence support the recognition of a new species of *Pseudocorynopoma* (Characidae: Corynopomini). Journal of Fish Biology 98(1): 219–236. https://doi.org/10.1111/jfb.14572

Menezes NA, Weitzman SH (2011) A systematic review of *Diapoma* (Teleostei: Characiformes: Characidae: Stevardiinae: Diapomini) with descriptions of two new species from southern Brazil. Papéis Avulsos de Zoologia 51(5): 59–82. https://doi.org/10.1590/S0031-10492011000500001

Miller MA, Pfeiffer W, Schwartz T (2010) Creating the CIPRES Science Gateway for inference of large phylogenetic trees. 2010 Gateway Computing Environments Workshop (GCE), 8 pp. https://doi.org/10.1109/GCE.2010.5676129

Mirande JM (2019) Morphology, molecules and the phylogeny of Characidae (Teleostei, Characiformes). Cladistics 35(3): 282–300. https://doi.org/10.1111/cla.12345

Moritz C (1994) Defining 'Evolutionarily Significant Units' for conservation. Trends in Ecology & Evolution 9: 373–375. https://doi.org/https://doi.org/10.1016/0169-5347(94)90057-4

Muniz P, Venturini N, Brugnoli E, Gutiérrez JM, Acuña A (2019) Chapter 30 – Río de la Plata: Uruguay. In: Sheppard C (Ed.) World Seas: An Environmental Evaluation (2nd edn.). Academic Press, 703–724. https://doi.org/10.1016/B978-0-12-805068-2.00036-X

Nei M (1987) Molecular Evolutionary Genetics. Columbia University Press, New York, 514 pp. https://doi.org/10.7312/nei-92038

Nei M, Li WH (1979) Mathematical model for studying genetic variation in terms of restriction endonucleases. Proceedings of the National Academy of Sciences of the United States of America 76(10): 5269–5273. https://doi.org/10.1073/pnas.76.10.5269

Paullier S, Bessonart J, Brum E, Loureiro M (2019) Lista de especies de peces de la cuenca del Río Queguay, Río Uruguay bajo. Boletin de la Sociedad Zoológica del Uruguay 28: 66–78. https://doi.org/10.26462/28.2.3

Pereira LHG, Maia GMG, Hanner R, Foresti F, Oliveira C (2011a) DNA barcodes discriminate freshwater fishes from the Paraíba do Sul River Basin, São Paulo, Brazil. Mitochondrial DNA 22(sup1): 71–79. https://doi.org/10.3109/19401736.2010.532213

Pereira LHG, Pazian MF, Hanner R, Foresti F, Oliveira C (2011b) DNA barcoding reveals hidden diversity in the Neotropical freshwater fish *Piabina argentea* (Characiformes: Characidae) from the Upper Paraná Basin of Brazil. Mitochondrial DNA 22(sup1): 87–96. https://doi.org/10.3109/19401736.2011.588213

Pereira LHG, Hanner R, Foresti F, Oliveira C (2013) Can DNA barcoding accurately discriminate megadiverse Neotropical freshwater fish fauna? BMC Genetics 14(1): 1–20. https://doi.org/10.1186/1471-2156-14-20

Pigott TD (2001) A review of methods for missing data. Educational Research and Evaluation 7(4): 353–383. https://doi.org/10.1076/edre.7.4.353.8937

Plavan AA, Passadore C, Gimenez LJ (2010) Fish assemblage in a temperate estuary on the uruguayan coast: Seasonal variation and

environmental influence. Brazilian Journal of Oceanography 58(4): 299–314. https://doi.org/10.1590/S1679-87592010000400005

Protogino LC, Miquelarena AM (2012) *Cyanocharax alburnus* (Hensel, 1870) (Characiformes: Characidae): First distribution record in Argentina. Check List 8(3): 581–583. https://doi.org/10.15560/8.3.581

Quinn GP, Keough MJ (2002) Experimental desing and data analysis for biologist. Cambrigde University Press, Cambrigde.

Rambaut A (2018) FigTree: Tree figure drawning tool. 1.4.4 ed, Institute of Evolutionary Biology, University of Edinburgh.

Rambaut A, Drummond AJ, Xie D, Baele G, Suchard MA (2018) Posterior summarization in bayesian phylogenetics using Tracer 1.7. Systematic Biology 67(5): 901–904. https://doi.org/10.1093/sysbio/syy032

Rodrigues-Oliveira IH, Kavalco KF, Pasa R (2023) Body shape variation in the Characid *Psalidodon rivularis* from São Francisco river, Southeast Brazil (Characiformes: Stethaprioninae). Acta Zoologica 104(3): 345–354. https://doi.org/10.1111/azo.12415

Ronquist F, Teslenko M, van der Mark P, Ayres DL, Darling A, Höhna S, Larget B, Liu L, Suchard MA, Huelsenbeck JP (2012) MrBayes 3.2: Efficient Bayesian phylogenetic inference and model choice across a large model space. Systematic Biology 61(3): 539–542. https://doi.org/10.1093/sysbio/sys029

Rosso JJ, Mabragaña E, González Castro M, Díaz de Astarloa JM (2012) DNA barcoding Neotropical fishes: Recent advances from the Pampa Plain, Argentina. Molecular Ecology Resources 12(6): 999–1011. https://doi.org/10.1111/1755-0998.12010

Rozas J, Ferrer-Mata A, Sánchez-DelBarrio JC, Guirao-Rico S, Librado P, Ramos-Onsins SE, Sánchez-Gracia A (2017) DnaSP 6: DNA Sequence Polymorphism Analysis of Large Data Sets. Molecular Biology and Evolution 34(12): 3299–3302. https://doi.org/10.1093/molbev/msx248

Sabaj MH (2020) Codes for natural history collections in ichthyology and herpeteology. Copeia 108(3): 593–669. https://doi.org/10.1643/ASIHCODONS2020

Serrano ÉA, Melo BF, Freitas-Souza D, Oliveira MLM, Utsunomia R, Oliveira C, Foresti F (2019) Species delimitation in Neotropical fishes of the genus *Characidium* (Teleostei, Characiformes). Zoologica Scripta 48(1): 69–80. https://doi.org/10.1111/zsc.12318

Silva-Santos R, de Barros Machado C, Zanata AM, Camelier P, Galetti Jr PM, Domingues de Freitas P (2023) Molecular characterization of *Astyanax* species (Characiformes: Characidae) from the upper Paraguaçu River basin, a hydrographic system with high endemism. Neotropical Ichthyology 21(2): e230032. https://doi.org/10.1590/1982-0224-2023-0032

Stockwell CA, Heilveil JS, Purcell K (2013) Estimating divergence time for two evolutionarily significant units of a protected fish species. Conservation Genetics 14(1): 215–222. https://doi.org/10.1007/s10592-013-0447-1

Tamura K, Stecher G, Kumar S (2021) MEGA11: Molecular Evolutionary Genetics Analysis Version 11. Molecular Biology and Evolution 38(7): e30223027. https://doi.org/10.1093/molbev/msab120

Taylor WR, Dyke GCV (1985) Revised procedures for staining and clearing small fishes and other vertebrates for bone and cartilage study. Cybium 9: 107–119.

Thomaz AT, Arcila D, Ortí G, Malabarba LR (2015) Molecular phylogeny of the subfamily Stevardiinae Gill, 1858 (Characiformes: Characidae): classification and the evolution of reproductive traits. BMC Evolutionary Biology 15(1): e146. https://doi.org/10.1186/s12862-015-0403-4

Thomaz AT, Malabarba LR, Knowles LL (2017) Genomic signatures of paleodrainages in a freshwater fish along the southeastern coast of Brazil: Genetic structure reflects past riverine properties. Heredity 119(4): 287–294. https://doi.org/10.1038/hdy.2017.46

Vanegas-Ríos JA, Azpelicueta MM, Malabarba LR (2018) A new species of *Diapoma* (Characiformes, Characidae, Stevardiinae) from the Rio Paraná basin, with an identification key to the species of the genus. Journal of Fish Biology 93(5): 830–841. https://doi.org/10.1111/jfb.13786

Vanegas-Rios JA, Britzke R, Mirande JM (2019) Geographic variation of *Moenkhausia bonita* (Characiformes: Characidae) in the rio de la Plata basin, with distributional comments on *M. intermedia*. Neotropical Ichthyology 17(1): e170123. https://doi.org/10.1590/1982-0224-20170123

Ward Jr JH (1963) Hierarchical grouping to optimize an objective function. Journal of the American Statistical Association 58(301): 236–244. https://doi.org/10.1080/01621459.1963.10500845

Ward RD (2009) DNA barcode divergence among species and genera of birds and fishes. Molecular Ecology Resources 9(4): 1077–1085. https://doi.org/10.1111/j.1755-0998.2009.02541.x

Zarucki M, González-Bergonzoni I, Teixeira-de-Mello F, Duarte A, Serra S, Quintans F, Loureiro M (2010) New records of freshwater fish for Uruguay. Check List 6(2): 1–4. https://doi.org/10.15560/6.2.191

Supplementary material 1

All COI sequences analyzed in the present work

Authors: James Anyelo Vanegas-Ríos, Wilson Sebastián Serra Alanís, María de las Mercedes Azpelicueta, Thomas Litz, Luiz Roberto Malabarba

Data type: xlsx

Link: https://doi.org/10.3897/zse.100.112778.suppl1

Supplementary material 2

Scree plots obtained from the morphometric and meristic data analyzed

Authors: James Anyelo Vanegas-Ríos, Wilson Sebastián Serra Alanís, María de las Mercedes Azpelicueta, Thomas Litz, Luiz Roberto Malabarba

Data type: pdf

Link: https://doi.org/10.3897/zse.100.112778.suppl2

Supplementary material 3

Total variance accounted for the PCA performed for the morphometric and meristic data

Authors: James Anyelo Vanegas-Ríos, Wilson Sebastián Serra Alanís, María de las Mercedes Azpelicueta, Thomas Litz, Luiz Roberto Malabarba
Data type: pdf

Link: https://doi.org/10.3897/zse.100.112778.suppl3

Supplementary material 4

Cluster analysis (Ward's method) of size-corrected morphometric data of analyzed specimens of *Diapoma pampeana*

Authors: James Anyelo Vanegas-Ríos, Wilson Sebastián Serra Alanís, María de las Mercedes Azpelicueta, Thomas Litz, Luiz Roberto Malabarba
Data type: tif

Link: https://doi.org/10.3897/zse.100.112778.suppl4

Supplementary material 5

Tukey box plot of most distinctive meristic data observed in analyzed specimens of *Diapoma pampeana*

Authors: James Anyelo Vanegas-Ríos, Wilson Sebastián Serra Alanís, María de las Mercedes Azpelicueta, Thomas Litz, Luiz Roberto Malabarba
Data type: pdf

Link: https://doi.org/10.3897/zse.100.112778.suppl5

Supplementary material 6

Uncorrected pairwise genetic distances using the COI data matrix

Authors: James Anyelo Vanegas-Ríos, Wilson Sebastián Serra Alanís, María de las Mercedes Azpelicueta, Thomas Litz, Luiz Roberto Malabarba
Data type: xlsx

Link: https://doi.org/10.3897/zse.100.112778.suppl6

Supplementary material 7

Haplotype network of the COI data analyzed of *D. pampeana*

Authors: James Anyelo Vanegas-Ríos, Wilson Sebastián Serra Alanís, María de las Mercedes Azpelicueta, Thomas Litz, Luiz Roberto Malabarba
Data type: pdf

Link: https://doi.org/10.3897/zse.100.112778.suppl7

Supplementary material 8

Table of coordinates used

Authors: James Anyelo Vanegas-Ríos, Wilson Sebastián Serra Alanís, María de las Mercedes Azpelicueta, Thomas Litz, Luiz Roberto Malabarba
Data type: xlsx

Link: https://doi.org/10.3897/zse.100.112778.suppl8